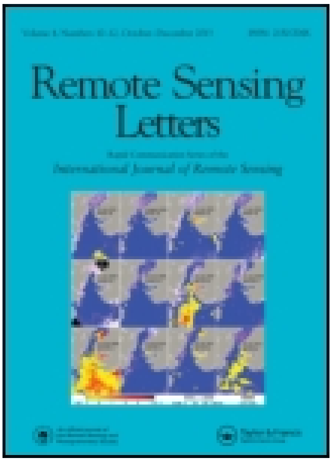

Remote Sensing Letters
Publication details, including instructions for authors and subscription information:
http://www.tandfonline.com/loi/trsl20

Results of the Global WaterPack: a novel product to assess inland water body dynamics on a daily basis

Igor Klein[a], Andreas Dietz[a], Ursula Gessner[a], Stefan Dech[a] & Claudia Kuenzer[a]

[a] German Remote Sensing Data Center, DFD, German Earth Observation Center, EOC, German Aerospace Center, DLR, Oberpfaffenhofen, Germany

Published online: 23 Jan 2015.

Remote Sensing Letters, 2015
Vol. 6, No. 1, 78–87, http://dx.doi.org/10.1080/2150704X.2014.1002945

Results of the Global WaterPack: a novel product to assess inland water body dynamics on a daily basis

Igor Klein*, Andreas Dietz, Ursula Gessner, Stefan Dech, and Claudia Kuenzer

German Remote Sensing Data Center, DFD, German Earth Observation Center, EOC, German Aerospace Center, DLR, Oberpfaffenhofen, Germany

(*Received 22 September 2014; accepted 20 December 2014*)

The understanding and assessment of surface water variability of inland water bodies, for example, due to climate variability and human impact, requires steady and continuous information about its inter- and intra-annual dynamics. In this letter, we present an approach using dynamic threshold techniques and utilizing time series to generate a data set containing detected surface water bodies on a global scale with daily temporal resolution. Exemplary results for the year 2013 that were based on moderate resolution imaging spectroradiometer products are presented in this letter. The main input data sets for the presented product were *MOD09GQ/MYD09GQ* and *MOD10A1/MYD10A1* with a spatial resolution of 250 m and 500 m, respectively. Using the static water mask *MOD44W*, we extracted training pixels to generate dynamic thresholds for individual data sets on daily basis. In a second processing step, the generated sequences of water masks were utilized to interpolate the results for any missing observations, either due to cloud coverage or missing data, as well as to reduce misclassification due to cloud shadow. The product provides an opportunity for further research and for assessing the drivers of changes of inland water bodies at a global scale.

1. Introduction

The quantification of the areal extent of inland water bodies has become an important topic over the last few years (Hinzman et al. 2005). Climate variability, changing environmental conditions and extensive utilization of inland waters by human activities, as well as varying meteorological conditions, have resulted in very strong inter- and intra-annual variability of inland water bodies in many regions (e.g. Feng et al. 2012; Kuenzer 2013; Micklin 2007). In the framework of the Global Climate Observation System (GCOS), lakes have been identified as one of the essential climate variables (ECV). Therefore, current and historical information is required for assessing the variability of water bodies in the context of the United Nations Framework Convention on Climate Change (UNFCC) and the Intergovernmental Panel on Climate Change (IPCC) (Organization and Commission 2011). Recent increase in availability and improved open access to large remote sensing data sets with high temporal resolution provides new opportunities to analyse inter- and intra-annual variability and long-term changes of inland water bodies. However, such data analysis also presents a number of challenges related to the utilization of such a large amount of data.

There are many global data sets that provide accurate information about the spatial distribution of lakes and water bodies. Such data sets include the Global Lakes and Wetlands Dataset (GLWD) (Lehner and Döll 2004), Shuttle Radar Topography Mission

*Corresponding author. Email: igor.klein@dlr.de

(SRTM) waterbody data (SWBD) (Slater et al. 2006), the latest 250 m moderate resolution imaging spectroradiometer (MODIS) water mask (Carroll et al. 2009) and the new high spatial resolution Global Water Bodies (GLOWABO) data set (Verpoorter et al. 2014). These data sets are very valuable, but provide only static information, thus showing only one temporal snap shot. Recently, many studies have been published dealing with the reconstruction of the historical evaluation of inland water bodies on regional scale based on temporal composites. Temporal composites usually contain best possible observation during a defined time period or the averaged values of clear sky observation for the defined time period. For example, Haas, Bartholomé, and Combal (2009), Bartholomé and Combal (2006) presented a Small Water Bodies product for the African continent that is based on the Satellite Pour l'Observation de la Terre (SPOT) data with 1 km spatial resolution. Fichtelmann and Borg (2012) demonstrated a self-learning algorithm based on multispectral data sets of the advanced along-track scanning radiometer (AATSR) for some test regions. Klein et al. (2014) analysed seasonal water bodies extent in Central Asia based on MODIS and advanced very high resolution radiometer (AVHRR) data. Pekel et al. (2014) presented a water surface detection scheme based on hue saturation value (HSV) transformation for 10-day composited MODIS multispectral data for the African continent.

Reliable information about the variability in the spatial distribution of inland water bodies such as natural lakes and artificial reservoirs is essential for diverse scientific disciplines such as water research management, climate and hydrology modelling, environmental change, agricultural management (Sun et al. 2012). Furthermore, lakes and reservoirs are important sinks of reactive nitrogen (Harrison et al. 2009) and sources of carbon dioxide as well as burial of organic carbon in sediments on a global scale (Verpoorter, Kutser, and Tranvik 2012). The objective of our work is to assess the dynamic nature of inland water bodies globally on a daily basis and to generate a data set that contains information on the temporal spatial variability of inland water bodies and inundated areas. For this purpose, we exploit the freely available MODIS data sets. The MODIS instrument on board of Terra and Aqua satellites provides imagery with daily temporal resolution on a global scale since 1999 and 2002, respectively. Monitoring water dynamics with such high-frequency imagery can provide important new insights on variability characteristics of lakes, reservoirs and regularly flooded areas. Especially as many changes owing to environmental change, climate variability or human influences might occur as subtle rather than abrupt changes. Therefore, the detectability of their gradual transition character may not be possible with temporal composites and lower temporal frequency. In this letter, we present our preliminary approach and results for the year 2013 and discuss achievements, challenges and further ongoing work.

2. Data

The presented work includes more than 200 MODIS tiles that cover mainland masses on global scale excluding the Polar Regions and very small islands across open oceans. The Polar Regions were excluded due to polar night and frequent cloud coverage; resulting in lack of clear sky observations. We used the following MODIS products: (i) daily near infrared (NIR) reflectance from *MODGQ09* and *MYD09GQ* with a spatial resolution of 250 m, (ii) daily 500 m snow cover product *MOD10A1* and *MYD10A1*, (iii) new static water mask *MOD44W* with a spatial resolution of 250 m. The *09GQ* data sets are distributed as gridded level 2 geo-corrected (L2G) products and contain atmospherically corrected surface reflectance at 620–670 nm (band 1) and 841–876 nm (band 2) spectra (Vermote and Vermeulen 1999). The *10A1* data sets are distributed as L3G products containing thematic information such as daily cloud coverage and snow coverage, as well as static information of oceans and inland lakes (Riggs, Hall, and Salomonson 2006). The land–water mask presented by Carroll et al. (2009) was generated based on the SWBD data set for areas between 60° S and 60° N, and 250 m global 16-day composite collection of 8+ years of Terra MODIS data and 6+ years of Aqua MODIS data. All MODIS products are delivered in sinusoidal projection. Furthermore, we used a global digital terrain model (DTM) with a spatial resolution of 90 m (CGIAR-CSI 2008).

3. Image processing

Pre-processing: The DTM data sets were first mosaicked on a continental scale and re-projected to sinusoidal projection. Next, the mosaics were clipped to the MODIS tiles and resampled to 250 m pixel resolution. Lastly, slopes of terrain were calculated using the maximal changes in elevation values of the DTM based on a 3 × 3 pixel moving window. The *MOD10A1* and *MYD10A1* were resampled from 500 m to 250 m resolution to enable pixel-based analysis based on all input data sets.

3.1. Water detection

In general, the unique spectral characteristic of water is that it has a very low reflection in the NIR spectra compared to most other surfaces. This feature has been utilized to detect water in a range of different approaches such as single band slicing, difference model, ratio model (Sheng and Su 1998), index model (Gao 1996; Ji, Zhang, and Wylie 2009; McFeeters 1996; Xu 2006) or a specific combination of these models (Martinis et al. 2013; Ouma and Tateishi 2006; Sun, Yu, and Goldberg 2011). Due to the immense data load and the resulting time-consuming process required at a global scale, we choose to use a single-band slicing approach based on dynamic calculation for each day and individual MODIS tiles. The utilization of a single-band method for water classification has been widely applied because it is straightforward to use and less time consuming compared to other methods (Feyisa et al. 2014; Ji, Zhang, and Wylie 2009; Ryu, Won, and Min 2002).

Fichtelmann and Borg (2012) introduced a self-learning algorithm for water mask extraction from multispectral AATSR data based on a static water mask. We followed a similar approach to derive dynamic thresholds for individual time steps and multiple time steps operating on a static water mask as a priori knowledge. The use of a dynamic threshold for individual data sets has many reasons as there are several different physical and biological factors that complicate the delineation of water and non-water pixels. For example, the spectral characteristics of a given waterbody can differ significantly depending on different water conditions, such as chlorophyll content, suspended particles, surface roughness and water depth. In addition, there are uncertainties in the atmospheric corrected product and other sources of errors unrelated to atmospheric correction (Vermote and Kotchenova 2008). This might result that a given pixel has different spectral values at different time steps. Cloud contamination and haze can also affect the detected spectral reflectance across scenes (Fichtelmann and Borg 2012). Therefore, a single threshold value derived for one image might not be suitable for another.

The presented classification approach is divided in two main modules as illustrated in Figure 1 (blue colour for water delineation and green colour for utilizing the generated sequence of water masks). Within the first classification step, we extract training pixels from the static water mask *MOD44W* and exclude cloud covered pixels, pixels flagged as ocean, lake ice, no data and pixels with outlined higher NIR reflectance for the considered

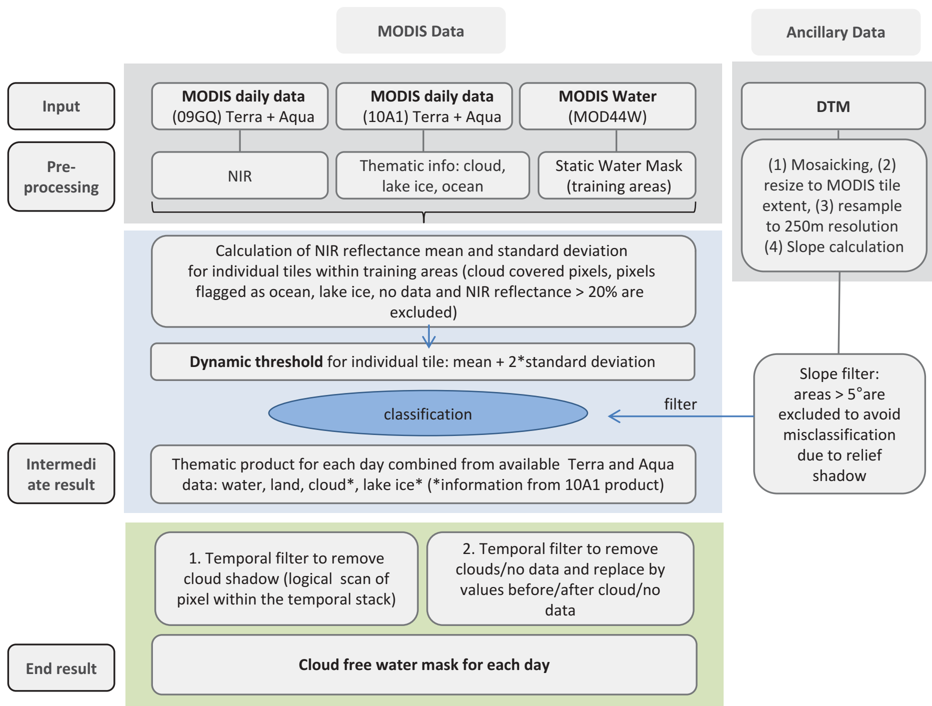

Figure 1. Preliminary workflow Global WaterPack 2013.

day and data set. This rule also excludes possible dried out areas that are flagged as water in *MOD44W* but feature higher NIR reflectance values (e.g. owing to changes in land cover caused by drying out or lake shrinkage). The algorithm operates on each individual MODIS tile so that regional differences are not smoothed. Based on the extracted set of training pixels, mean and standard deviation of NIR reflectance are calculated. The mean value plus standard deviation for the individual day and tile is finally used as the dynamic single band threshold for decision tree water classification on the considered day and tile. The standard deviation accounts for situations that differ from 'normal' conditions. In this way, temporal difference in spectral variations (e.g. owing to higher sediment load or algae content) along with across scene differences in atmospheric conditions are taken into account. Therefore, pixels comprising shallow water are also classified as water as the dynamic threshold increases. In flooding situations, we expect increased sediment load within extracted training pixels and therefore a higher threshold that enable the detection of seasonal inundation and flooded areas. A minimum size of five pixels was set to avoid noise effects by single pixels (McCullough, Loftin, and Sader 2012). This approach is applied for Terra (MOD) and Aqua (MYD) data sets that are subsequently combined for detected water pixels resulting in one water mask for each day.

One of the main misclassifications of water bodies occurs in mountainous regions, where relief shadows feature similar spectral reflectance in NIR as water (McCullough, Loftin, and Sader 2012). The knowledge about the fact that water bodies do not exist on steep slopes is utilized to avoid the misclassification in these regions. According to Niu et al. (2009), 99.2% of wetlands and water bodies in China are located on areas with slope less than 8° and 97.5% with a slope less than 5°. We assume that this is also true for other regions and apply 5° of inclination as a threshold to avoid misclassification resulting from the relief shadow effect.

3.2. Temporal interpolation

The presence of cloud shadow and its misclassification as water cannot be solved using only single-band threshold method of optical sensors. We assume that the probability of cloud shadows located over a given pixel within a certain time interval is very low and is therefore a 'short-term condition'. Therefore, we applied a temporal filter excluding all pixels that are classified as water only once in a time interval of t_0 ±4 days (the considered time interval of 9 days is following MODIS 8 day composite products as a minimum time interval) relatively to the given pixel. After filtering out the errors caused by cloud shadow, we interpolate the results for those pixels that were either cloud covered or flagged as no data. Here, the classification of water or no-water from temporally closest clear sky observation is used to fill the gaps resulting from cloud coverage or no data. As this approach might generate some misclassifications, especially in regions with persistent and long cloud coverage or polar night, we provide an assessment layer that contains the information on how often a pixel was covered by cloud or flagged as no data. This information should assist in the better interpretation of generated results.

4. Results and discussion

In total over 200 MODIS tiles were calculated including around 292,000 input data sets. As it is not possible to visualize the variability on a global scale, we present selected examples to demonstrate the detected intra-annual dynamics. Preliminary results for six different sites for the year 2013 are illustrated in Figure 2. The examples demonstrate intra-annual variability of selected inland water bodies and inundated areas. It underlines that the presented approach is capable to capture seasonal water coverage of lakes and reservoirs as well as flooding events. The first example illustrates a floodplain located on the right bank of the Amazonas River, Brazil (*a*). This complex system of river, channels and around 30 lakes has an open surface water areal extent varying between 600 and 2500 km^2 (Bourgoin et al. 2007). The shrinking southern.

Aral Sea, Uzbekistan (*b*) shows some areas that were temporally flooded in 2013. In this flat terrain, the discharge from the river Amu Darya still reaches the lake during spring time because of snow melt from the Pamir Mountains. During hot summers usually no waters reach the southern Aral Sea due to upstream water consumption resulting in high water loss and shrinkage of the water surface area (Micklin 2007). The third example shows the American Falls Reservoir located in north-western USA (*c*). The reservoir stores snowmelt water in the spring (Allen and Tasumi 2005) that is subsequently used for irrigation during the growing season resulting in steady shrinkage of the reservoirs water surface area. Lake Liambezi and Chobe floodplain (*d*) in eastern Caprivi (Namibia) show large temporal flooded areas occurring in the rainy season. The regular flooding during recent years has caused re-emergence of perennial lakes and wetlands that had dried out due to a drought between 1980 and 1990 (Long, Fatoyinbo, and Policelli 2014). Lake Tuz (*e*) in Turkey is a large hyper-saline lake without a natural outlet and is mainly fed by rainfall and ground water. Most parts of this lake are seasonally flooded during winter, but dry up in summer due to evaporation (Yildiz and Sinan 2010). The last example, the Dongting Lake, China (*f*) features strong surface variability depending on discharge from

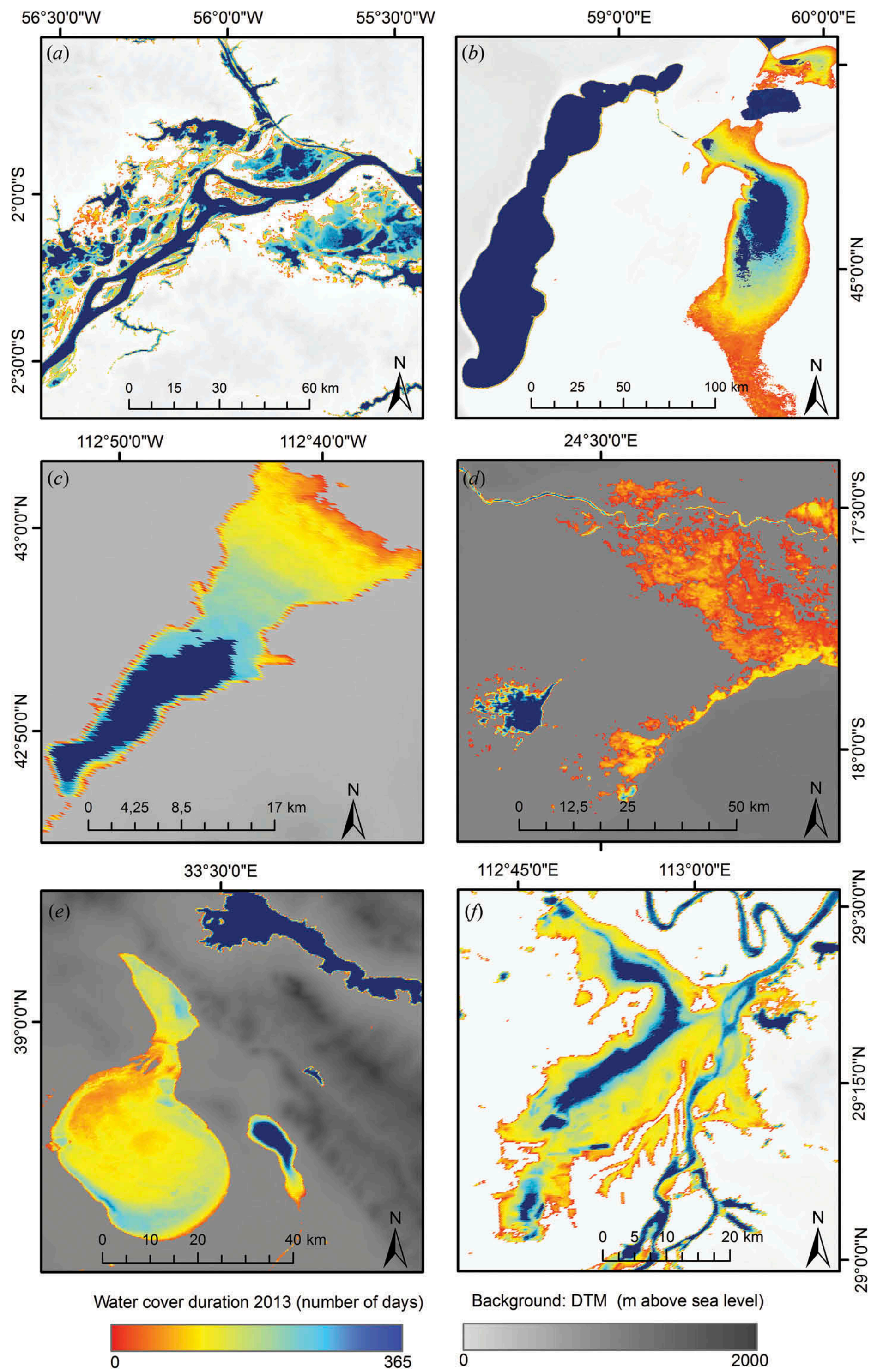

Figure 2. Water cover duration based on preliminary results for the year 2013. Number of days that were detected as water for each pixel. (*a*) Floodplain lakes along Amazonas (Brasil), (*b*) Southern Aral Sea (Uzbekistan), (*c*) American Falls Reservoir (USA), (*d*) Lake Liambezi (Namibia), (*e*) Lake Tuz (Turkey), (*f*) Dongting Lake (China). Projection: GCS WGS 1984.

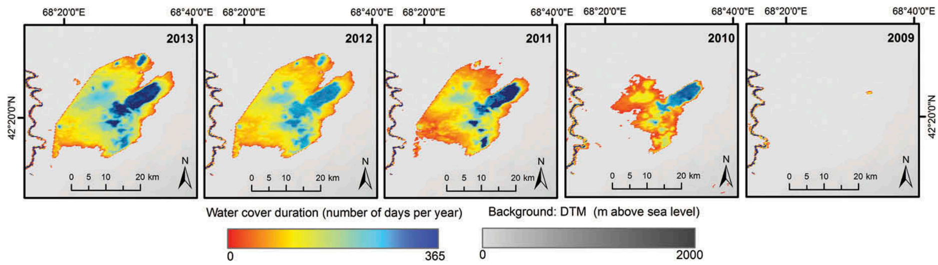

Figure 3. Detected water cover duration for Koksaray Reservoir, Kazakhstan for the year 2009–2013. Projection: GCS WGS 1984.

several rivers. The Dongting Lake can expand to 2691 km^2 during annual floods and shrink to 710 km^2 during dry season (Du et al. 2001).

Figure 3 demonstrates the Koksaray Reservoir, Kazakhstan and its intra- and inter-annual variability. The reservoir was recently constructed with purpose of flood protection and irrigation agriculture.

The discussed results illustrate that the approach is capable to detect seasonal and inter-annual changes in water extent. According to visual comparison with the original data the derived water masks represented the real water surface extent for specific events such as inundation, as well as variability during rainy and dry season. First validation efforts were made by comparing the results with water masks derived semi-automatically from higher spatial resolution optical data (40 Landsat images with spatial resolution of 30 m) for different time steps and different test sides. The Landsat images were segmented and classified in water and no-water using multispectral information and normalised difference water index. The plausibility of the high-resolution water masks were checked manually. The exemplary assessment showed reasonable results averaging 89% agreement in detected water pixels between our results and water masks derived from Landsat images. A systematic validation is being performed and will be presented after final stage. We also intend to compare the results with existing near real time flood services data. We observed an overestimation owing to the coarse pixel size (250 m), as well as misclassification of dark land cover surfaces such as volcanic materials (e.g. volcanic ashes, basalt), dark needleleaved forest and relief shadow (below 5° inclination threshold). In high latitude areas, an overestimation was observed during winter season where low sun angles cause high degrees of shadow and therefore unfavourable satellite detection conditions. Underestimation was observed especially in areas that were covered by clouds for long time intervals waters with high sediment load, and swamps covered by floating vegetation.

5. Conclusion

In this letter, we presented our approach to detect water bodies on global scale at high temporal resolution based on medium-resolution remote sensing data and utilizing the time series of data. The presented examples illustrate that intra-annual variability of natural lakes, water reservoirs and flooded areas can be effectively captured. A systematic validation and reanalysis of entire available data set is being performed and will be published in near future. The approach allows fast processing using the NIR channel, thematic cloud cover information and a-priori knowledge from a static water mask.

Classification errors due to cloud shadows were corrected utilizing the time series of data. Misclassifications were found for land cover types with low NIR spectral reflectance. These misclassifications will be addressed in the future by integrating additional auxiliary data sets.

The presented examples demonstrate intra-annual variability of different inland water bodies systems and underline the value and potential of such information. The goal of our work is to develop a data set that includes inter- and intra-annual variability of inland water bodies on a global scale with high temporal resolution. The knowledge about beginning, ending and duration of inundation over dynamical lakes, reservoirs, wetlands and flooded areas might reveal new findings about ongoing environmental shifts. Certain relations, for example, the impact of El Nino-Southern Oscillation (ENSO) and other large scale weather patterns can be investigated with the focus on quantitative inland water variability. Future work will address extending the approach to the entire available time series of MODIS data, as well as on the elimination of misclassification errors caused by similarity in NIR spectra of other land cover types. For this purpose, additional MODIS products such as vegetation indices and thermal measurements will be included and utilized.

Acknowledgements

The authors would like to thank NASA, NOAA, USGS and NSIDC for providing comfortable download services and all data sets free of charge. Furthermore, we would like to thank the anonymous reviewers for their valuable and constructive comments on the manuscript.

References

Allen, R., and M. Tasumi. 2005. “Evaporation from American Falls Reservoir in Idaho Via a Combination of Bowen Ratio and Eddy Covariance.” *Impacts of Global Climate Change* 1–17. doi:10.1061/40792(173)527.

Bartholomé, E., and B. Combal. 2006. “Small Water Bodies.” In *VGT4Africa User Manual*, 1st ed., edited by E. Bartholomé. Luxembourg: Office for Official Publication of the European Communities.

Bourgoin, L. M., M.-P. Bonnet, J.-M. Martinez, P. Kosuth, G. Cochonneau, P. Moreira-Turcq, J.-L. Guyot, P. Vauchel, N. Filizola, and P. Seyler. 2007. “Temporal Dynamics of Water and Sediment Exchanges between the Curuaí Floodplain and the Amazon River, Brazil.” *Journal of Hydrology* 335: 140–156. doi:10.1016/j.jhydrol.2006.11.023.

Carroll, M. L., J. R. Townshend, C. M. DiMiceli, P. Noojipady, and R. A. Sohlberg. 2009. “A New Global Raster Water Mask at 250 m Resolution.” *International Journal of Digital Earth* 2: 291–308. doi:10.1080/17538940902951401.

CGIAR-CSI (Consultative Group on International Agricultural Research–Consortium for Spatial Information). 2008. Accessed April 17, 2014. http://srtm.csi.cgiar.org/

Du, Y., S. Cai, X. Zhang, and Y. Zhao. 2001. “Interpretation of the Environmental Change of Dongting Lake, Middle Reach of Yangtze River, China, by 210 Pb Measurement and Satellite Image Analysis.” *Geomorphology* 41 (2001): 171–181.

Feng, L., C. Hu, X. Chen, X. Cai, L. Tian, and W. Gan. 2012. “Assessment of Inundation Changes of Poyang Lake Using MODIS Observations between 2000 and 2010.” *Remote Sensing of Environment* 121: 80–92. doi:10.1016/j.rse.2012.01.014.

Feyisa, G. L., H. Meilby, R. Fensholt, and S. R. Proud. 2014. “Automated Water Extraction Index: A New Technique for Surface Water Mapping Using Landsat Imagery.” *Remote Sensing of Environment* 140: 23–35. doi:10.1016/j.rse.2013.08.029.

Fichtelmann, B., and E. Borg. 2012. “A New Self-Learning Algorithm for Dynamic Classification of Water Bodies.” In *Proceedings of Computational Science and Its Applications - ICCSA 2012, Part III, 12th International Conference*, Salvador de Bahia, edited by B. Murgante, O. Gervasi,

S. Misra, N. Nedjah, A. M. A. C. Rocha, D. Taniar, and B. O. Apduhan, 457–470. Salvador de Bahia: Springer.
Gao, B. 1996. "NDWI a Normalized Difference Water Index for Remote Sensing of Vegetation Liquid Water from Space." *Remote Sensing of Environment* 58: 257–266.
Haas, E. M., E. Bartholomé, and B. Combal. 2009. "Time Series Analysis of Optical Remote Sensing Data for the Mapping of Temporary Surface Water Bodies in Sub-Saharan Western Africa." *Journal of Hydrology* 370: 52–63. doi:10.1016/j.jhydrol.2009.02.052.
Hall, D. K., and G. A. Riggs. 2007. "Accuracy Assessment of the MODIS Snow Products." *Hydrological Processes* 21: 1534–1547. doi:10.1002/hyp.
Harrison, J. A., R. J. Maranger, R. B. Alexander, A. E. Giblin, P.-A. Jacinthe, E. Mayorga, S. P. Seitzinger, D. J. Sobota, and W. M. Wollheim. 2009. "The Regional and Global Significance of Nitrogen Removal in Lakes and Reservoirs." *Biogeochemistry* 93: 143–157. doi:10.1007/s10533-008-9272-x.
Hinzman, L. D., N. D. Bettez, W. R. Bolton, F. S. Chapin, M. B. Dyurgerov, C. L. Fastie, B. Griffith, R. D. Hollister, A. Hope, H. P. Huntington, A. M. Jensen, G. J. Jia, T. Jorgenson, D. L. Kane, D. R. Klein, G. Kofinas, A. H. Lynch, A. H. Lloyd, A. D. McGuire, F. E. Nelson, W. C. Oechel, T. E. Osterkamp, C. H. Racine, V. E. Romanovsky, R. S. Stone, D. A. Stow, M. Sturm, C. E. Tweedie, G. L. Vourlitis, M. D. Walker, D. A. Walker, P. J. Webber, J. M. Welker, K. S. Winker, and K. Yoshikawa. 2005. "Evidence and Implications of Recent Climate Change in Northern Alaska and Other Arctic Regions." *Climatic Change* 72: 251–298. doi:10.1007/s10584-005-5352-2.
Ji, L., L. Zhang, and B. Wylie. 2009. "Analysis of Dynamic Thresholds for the Normalized Difference Water Index." *Photogrammetric Engineering and Remote Sensing* 75 (11): 1307–1317.
Klein, I., A. J. Dietz, U. Gessner, A. Galayeva, A. Myrzakhmetov, and C. Kuenzer. 2014. "Evaluation of Seasonal Water Body Extents in Central Asia over the past 27 Years Derived from Medium-Resolution Remote Sensing Data." *International Journal of Applied Earth Observation and Geoinformation* 26: 335–349. doi:10.1016/j.jag.2013.08.004.
Kuenzer, C. 2013. "Threatening Tonle Sap : Challenges for Southeast Asia's Largest Freshwater Lake." *Pacific Geographies* 40: 29–31.
Lehner, B., and P. Döll. 2004. "Development and Validation of a Global Database of Lakes, Reservoirs and Wetlands." *Journal of Hydrology* 296: 1–22. doi:10.1016/j.jhydrol.2004.03.028.
Long, S., T. E. Fatoyinbo, and F. Policelli. 2014. "Flood Extent Mapping for Namibia Using Change Detection and Thresholding with SAR." *Environmental Research Letters* 9: 035002. doi:10.1088/1748-9326/9/3/035002.
Martinis, S., A. Twele, C. Strobl, J. Kersten, and E. Stein. 2013. "A Multi-Scale Flood Monitoring System Based on Fully Automatic MODIS and TerraSAR-X Processing Chains." *Remote Sensing* 5 (11): 5598–5619.
McCullough, I. M., C. S. Loftin, and S. A. Sader. 2012. "High-Frequency Remote Monitoring of Large Lakes with MODIS 500m Imagery." *Remote Sensing of Environment* 124: 234–241. doi:10.1016/j.rse.2012.05.018.
McFeeters, S. K. 1996. "The Use of the Normalized Difference Water Index (NDWI) in the Delineation of Open Water Features." *International Journal of Remote Sensing* 17: 1425–1432. doi:10.1080/01431169608948714.
Micklin, P. 2007. "The Aral Sea Disaster." *Annual Reviews Earth Planet Sciences* 35: 47–72. doi:10.1146/annurev.earth.35.031306.140120.
Niu, Z., P. Gong, X. Cheng, J. Guo, L. Wang, H. Huang, S. Shen, Y. Wu, X. Wang, X. Wang, Q. Ying, Q. Liang, L. Zhang, L. Wang, Q. Yao, Z. Yang, Z. Guo, and Y. Dai. 2009. "Geographical Characteristics of China's Wetlands Derived from Remotely Sensed Data." *Science in China Series D: Earth* Sciences 52: 723–738. doi:10.1007/s11430-009-0075-2.
Organization, W.M., Commission, I.O. 2011. *Systematic Observation Requirements for Satellite-Based Data Products for Climate - 2011 Update, GCOS - 154*. ed. Geneva: WMO GCOS.
Ouma, Y. O., and R. Tateishi. 2006. "A Water Index for Rapid Mapping of Shoreline Changes of Five East African Rift Valley Lakes: An Empirical Analysis Using Landsat TM and ETM+ Data." *International Journal of Remote Sensing* 27: 3153–3181. doi:10.1080/01431160500309934.
Pekel, J.-F., C. Vancutsem, L. Bastin, M. Clerici, E. Vanbogaert, E. Bartholomé, and P. Defourny. 2014. "A Near Real-Time Water Surface Detection Method Based on HSV Transformation of

MODIS Multi-Spectral Time Series Data." *Remote Sensing of Environment* 140: 704–716. doi:10.1016/j.rse.2013.10.008.
Riggs, G. A., D. K. Hall, and V. V. Salomonson. 2006. *MODIS Snow Products User Guide to Collection 5*. Boulder, CO: National Snow and Ice Data Center. Digital media.
Ryu, J.-H., J.-S. Won, and K. D. Min. 2002. "Waterline Extraction from Landsat TM Data in a Tidal Flat A Case Study in Gomso Bay, Korea." *Remote Sensing of Environment* 83: 442–456.
Sheng, Y., and Y. X. Q. Su. 1998. "Challenging the Cloud Contamination Problem in Flood Monitoring with NOAA/AVHRR Imagery." *Photogrammetry Engineering & Remote Sensing* 64: 191–198.
Slater, J. A., G. Garvey, C. Johnston, J. Haase, B. Heady, G. Kroenung, and J. Little. 2006. "The SRTM Data Finishing Process and Products." *Photogrammetric Engineering & Remote Sensing* 72 (3): 237–247. doi:10.14358/PERS.72.3.237.
Sun, D., Y. Yu, and M. D. Goldberg. 2011. "Deriving Water Fraction and Flood Maps From MODIS Images Using a Decision Tree Approach." *IEEE Journal of Selected Topics in Applied Earth Observations and Remote Sensing* 4: 814–825. doi:10.1109/JSTARS.2011.2125778.
Sun, F., W. Sun, J. Chen, and P. Gong. 2012. "Comparison and Improvement of Methods for Identifying Waterbodies in Remotely Sensed Imagery." *International Journal of Remote Sensing* 33: 6854–6875. doi:10.1080/01431161.2012.692829.
Vermote, E. F., and A. Vermeulen. 1999. "Algorithm Technical Background Document Atmospheric Correction Algorithm : Spectral Reflectances (MOD09) NASA Contract NAS5-96062." 1–107.
Vermote, E. F., and S. Kotchenova. 2008. "Atmospheric Correction for the Monitoring of Land Surfaces." *Journal of Geophysical Research* 113: D23S90. doi:10.1029/2007JD009662.
Verpoorter, C., T. Kutser, D. A. Seekell, and L. J. Tranvik. 2014. "A Global Inventory of Lakes Based on High-Resolution Satellite Imagery." *Geophysical Research Letters* 41 (22): 1–7. doi:10.1002/2014GL060641.
Verpoorter, C., T. Kutser, and L. Tranvik. 2012. "Automated Mapping of Water Bodies Using Landsat Multispectral Data." *Limnology and Oceanography: Methods* 10: 1037–1050. doi:10.4319/lom.2012.10.1037.
Xu, H. 2006. "Modification of Normalised Difference Water Index (NDWI) to Enhance Open Water Features in Remotely Sensed Imagery." *International Journal of Remote Sensing* 27: 3025–3033. doi:10.1080/01431160600589179.
Yildiz, M., and A. Sinan. 2010. "Evaluation of Geotechnical Properties of the Salt Layers on the Lake Tuz." *Scientific Research and Essays* 5 (18): 2656–2663.